

# Unified plastic-damage model for concrete and its applications to dynamic nonlinear analysis of structures

Jian-Ying Wu<sup>†</sup>

*Department of Civil Engineering, South China University of Technology, Guangzhou,  
Post code: 510640, P.R. China*

Jie Li<sup>‡</sup>

*Department of Building Engineering, Tongji University, Shanghai,  
Post code: 200092, P.R. China*

*(Received October 7, 2005, Accepted September 20, 2006)*

**Abstract.** In this paper, the energy-based plastic-damage model previously proposed by the authors [International Journal of Solids and Structures, 43(3-4): 583-612] is first simplified with an empirically defined evolution law for the irreversible strains, and then it is extended to its rate-dependent version to account for the strain rate effect. Regarding the energy dissipation by the motion of the structure under dynamic loadings, within the framework of continuum damage mechanics a new damping model is proposed and incorporated into the developed rate-dependent plastic-damage mode, leading to a unified constitutive model which is capable of directly considering the damping on the material scale. Pertinent computational aspects concerning the numerical implementation and the algorithmic consistent modulus for the unified model are also discussed in details, through which the dynamic nonlinear analysis of damping structures can be coped with by the same procedures as those without damping. The proposed unified plastic-damage model is verified by the simulations of concrete specimens under different quasi-static and high rate straining loading conditions, and is then applied to the Koyna dam under earthquake motions. The numerical predictions agree fairly well with the results obtained from experimental tests and/or reported by other investigators, demonstrating its capability for reproducing most of the typical nonlinear performances of concrete under quasi-static and dynamic loading conditions.

**Keywords:** concrete; continuum damage mechanics; nonlinear analysis; dynamics; damping.

---

## 1. Introduction

As we know, an undamped structure would vibrate freely and the magnitude of the oscillation would be constant if no energy-dissipation exists. However in reality, energy is inevitably dissipated by the motion of the structure and the magnitude of the oscillation steadily diminishes. Named as damping, this energy dissipation is of significant influence on the response of structures under dynamic loadings. In the literature, damping is generally considered via the classical Rayleigh

---

<sup>†</sup> Ph.D., Corresponding author, E-mail: [jywu@scut.edu.cn](mailto:jywu@scut.edu.cn)

<sup>‡</sup> Professor, E-mail: [lijie@mail.tongji.edu.cn](mailto:lijie@mail.tongji.edu.cn)

assumption where the damping matrix  $\Xi$  is the linear combination of the mass matrix  $\mathbf{M}$  and stiffness matrix  $\mathbf{K}$ , that is,

$$\Xi = \beta_{\mathbf{M}}\mathbf{M} + \beta_{\mathbf{K}}\mathbf{K} \quad (1)$$

where  $\beta_{\mathbf{M}}$  and  $\beta_{\mathbf{K}}$  are user-defined constants, related to the critical damping value  $\xi_i$  and the natural frequency  $\omega_i$  for a given mode  $i$  as

$$\xi_i = \frac{1}{2} \left( \frac{\beta_{\mathbf{M}}}{\omega_i} + \beta_{\mathbf{K}} \omega_i \right) \quad (2)$$

It is known that the mass-proportional damping matrix  $\beta_{\mathbf{M}}\mathbf{M}$  would introduce a physically inadmissible dissipation under rigid body motions, and it alone could not provide sufficient dissipation to suppress the high-frequency numerical noises even if the powerful HHT- $\alpha$  method (Hughes 1987) is used. Therefore, many researchers (El-Aidi and Hall 1989, Vargas-Loli and Fenves 1989, Bhattacharjee and Leeger 1993, Lee and Fenves 1998, Faria *et al.* 2002, etc.) adopted the stiffness-proportional damping matrix alone to consider the energy dissipation, that is

$$\Xi = \beta_{\mathbf{K}}\mathbf{K} \quad (3)$$

However, the key problem in dynamic nonlinear analysis is that the stiffness of structure would change with time as the material comes into nonlinearity, a constant stiffness matrix  $\mathbf{K}$  throughout would introduce fictitious damping forces that remain high on a finite element with vanishing stiffness (El-Aidi and Hall 1989), which is obviously not physically right. To solve the problem, various methods were proposed either by setting the damping to zero on a cracking element or by adopting the tangent matrix. Unfortunately, the former method would lead to the numerical problems of convergence and stability, and the later one would obtain negative damping when the material comes into softening regions. In fact, energy is mostly dissipated on the material scale, so it might be more consistent to consider damping by endowing a constitutive model with the capability of reproducing the appropriate energy dissipations.

In addition to the energy-dissipation, other issues such as the strain rate effect under high rate straining and the typical nonlinear behavior evidenced under quasi-static loading conditions should be also addressed appropriately in the dynamic nonlinear analysis. It is now generally accepted that the observed nonlinearities in concrete behavior are mainly attributed to two distinct microstructural changes: (i) the evolution of microcracks and/or microvoids and (ii) the shear slidings (plastic flows) along some preferred crack lips. Owing to the inherent capabilities of continuum damage mechanics (CDM) and plasticity of describing the above two mechanisms, different versions of combined plastic-damage models have been proposed to describe the nonlinearities of concrete since 1980s (Ortiz 1985, Simo and Ju 1987, Ju 1989, Lubliner *et al.* 1989, Yazdani and Schreyer 1990, Faria *et al.* 1998, etc.). Among others, an energy-based plastic-damage model (Li and Wu 2004, Wu and Li 2004, Wu *et al.* 2006) has recently been proposed for concrete, where the damage criteria is established based on the damage energy release rate (DERR) and the irreversible strain is described within the framework of effective space plasticity (Ju 1989). The model not only is thermodynamically consistent and computationally efficient but also is able to reproduce fairly well the typical experimental observations of concrete under quasi-static loadings, such as the stiffness degradation, the enhancement of strength and ductility under compressive confinement, the strength

decay induced by orthogonal tensile cracking, the unilateral effect under cyclic loading and the irreversible deformations upon unloading.

Due to its main intention for large time-consuming dynamic nonlinear analysis, in Section 2 of this paper the above plastic-damage model is first simplified with an empirically defined evolution law for irreversible strains, and is then extended into its rate-dependent version to embody the strain rate effect. Regarding the energy dissipations, a new damping model on the material scale is proposed and incorporated into the developed rate-dependent plastic-damage model within the framework of CDM, leading to a unified constitutive model to directly take the damping into consideration. Pertinent computational aspects concerning the numerical implementation and the algorithmic consistent modulus are discussed in details in Section 3, through which the dynamic nonlinear analysis of damping structures can be dealt with by the same procedures as those without damping. Section 4 is devoted to the validation of the proposed unified plastic-damage model by some experimental tests of concrete specimens under quasi-static and different rate straining loadings. In Section 5 the proposed unified model is applied to the dynamic nonlinear analysis of Koyna dam under earthquake excitation to further demonstrate its effectiveness and capability for the nonlinear analysis of concrete structures. Section 6 closes this paper with the most relevant conclusions.

## 2. Unified plastic-damage model for concrete

### 2.1 Basic idea

The governing motion equation for discretized structure due to the external specified ground accelerations  $\ddot{\mathbf{u}}_g$  and other static loadings  $\mathbf{F}^{\text{sta}}$  can be generally written as

$$\mathbf{M}\ddot{\mathbf{u}} + \mathbf{F}(\mathbf{u}, \dot{\mathbf{u}}) = -\mathbf{M}\mathbf{l}_g\ddot{\mathbf{u}}_g + \mathbf{F}^{\text{sta}} = \mathbf{F}^{\text{ext}} \quad (4)$$

where  $\mathbf{u}$ ,  $\dot{\mathbf{u}}$  and  $\ddot{\mathbf{u}}$  are the displacement, velocity and acceleration relative to  $\ddot{\mathbf{u}}_g$ ;  $\mathbf{l}_g$  is the influence matrix for  $\ddot{\mathbf{u}}_g$ ;  $\mathbf{F}^{\text{ext}} = -\mathbf{M}\mathbf{l}_g\ddot{\mathbf{u}}_g + \mathbf{F}^{\text{sta}}$  is the total external force vector.

In Eq. (4), the internal resisting force  $\mathbf{F}(\mathbf{u}, \dot{\mathbf{u}})$  consists of two parts: (i) the restoring force  $\mathbf{F}^{\text{res}}$ , expressed as function of the deformation in the structure

$$\mathbf{F}^{\text{res}}(\mathbf{u}) = \int_{\Omega} \mathbf{B}^T \boldsymbol{\sigma}(\mathbf{u}) d\Omega = \mathbf{K}(\mathbf{u})\mathbf{u} \quad (5)$$

and (ii) the damping force  $\mathbf{F}^{\text{vis}}$ , related to the deformation rate

$$\mathbf{F}^{\text{vis}}(\mathbf{u}, \dot{\mathbf{u}}) = \int_{\Omega} \mathbf{B}^T \boldsymbol{\sigma}_{\text{vis}}(\mathbf{u}, \dot{\mathbf{u}}) d\Omega = \boldsymbol{\Xi}(\mathbf{u}, \dot{\mathbf{u}})\dot{\mathbf{u}} \quad (6)$$

where  $\Omega$  is the finite element domains of the integral of the stress field;  $\mathbf{B}$  is the matrix form of the strain-displacement operator;  $\boldsymbol{\sigma}$  and  $\boldsymbol{\sigma}_{\text{vis}}$  are the Cauchy stress and the damping stress, respectively. Therefore,  $\mathbf{F}(\mathbf{u}, \dot{\mathbf{u}})$  can be rewritten as

$$\mathbf{F}(\mathbf{u}, \dot{\mathbf{u}}) = \int_{\Omega} \mathbf{B}^T (\boldsymbol{\sigma} + \boldsymbol{\sigma}_{\text{vis}}) d\Omega = \int_{\Omega} \mathbf{B}^T \boldsymbol{\sigma}_{\text{tot}} d\Omega \quad (7)$$

with  $\boldsymbol{\sigma}_{\text{tot}}$  being the total stress resulted from external loadings, expressed as

$$\boldsymbol{\sigma}_{\text{tot}} = \boldsymbol{\sigma} + \boldsymbol{\sigma}_{\text{vis}} \quad (8)$$

It will be shown later that it is not the total stress  $\boldsymbol{\sigma}_{\text{tot}}$ , but the Cauchy stress  $\boldsymbol{\sigma}$  alone which influences the damage evolution and other material nonlinear behavior, i.e. in one word, the damping stress is just the result but not the reason.

## 2.2 Energy based plastic-damage model

Theoretically, the above principle applies for many constitutive models, and it is thus possible to establish a unified one that directly takes the damping into consideration on the material scale. Here the energy-based rate-independent plastic-damage model previously proposed by the authors (Wu *et al.* 2006) is chosen as a start to develop such one. Basically, a tensile damage scalar  $d^+$  and a shear damage scalar  $d^-$  respectively corresponding to pure tension and pure compression, are adopted to describe the tensile and shear damage mechanisms that result in the degradation of macro-mechanical properties. The effective stress  $\bar{\boldsymbol{\sigma}}$  in damaged material is assumed to follow the classical elastoplastic behavior (Ju 1989, Faria *et al.* 1998), i.e.

$$\bar{\boldsymbol{\sigma}} = \mathbf{S}_0 : \boldsymbol{\varepsilon}^e = \mathbf{S}_0 : (\boldsymbol{\varepsilon} - \boldsymbol{\varepsilon}^p) \quad (9)$$

or equivalently

$$\boldsymbol{\varepsilon}^e = \mathbf{C}_0 : \bar{\boldsymbol{\sigma}} \quad (10)$$

where  $\mathbf{S}_0$  and  $\mathbf{C}_0 = \mathbf{S}_0^{-1}$  denote the usual fourth-order isotropic linear-elastic stiffness and compliance tensors, respectively;  $\boldsymbol{\varepsilon}$ ,  $\boldsymbol{\varepsilon}^e$  and  $\boldsymbol{\varepsilon}^p$  are all rank-two tensors, denoting the strain tensor, its elastic and plastic tensor components.

To determine the plastic strain  $\boldsymbol{\varepsilon}^p$ , the so-called ‘‘effective stress space plasticity’’ (Ju 1989), can be resorted to establish the evolution law for the plastic strains. Since the present unified model is mainly intended for large time-consuming dynamic analysis, here a simplified evolution law is postulated, in which the plastic strains are treated as an ‘‘overall effect’’ (Faria *et al.* 1998, Li and Wu 2004), i.e.

$$\dot{\boldsymbol{\varepsilon}}^p = \dot{\lambda} \bar{\boldsymbol{\sigma}} \quad (11)$$

with  $\dot{\lambda}$  being expressed as

$$\dot{\lambda} = E_0 [\xi^+ H(\dot{d}^+) + \xi^- H(\dot{d}^-)] \frac{\langle \boldsymbol{\varepsilon}^e : \dot{\boldsymbol{\varepsilon}} \rangle}{\bar{\boldsymbol{\sigma}} : \bar{\boldsymbol{\sigma}}} \geq 0 \quad (12)$$

where  $H(\cdot)$  is the Heaviside function and  $\langle x \rangle = (x + |x|)/2$  is the McAuley function;  $E_0$  denotes the Young’s modulus;  $0.0 \leq \xi^\pm \leq 1.0$  are parameters controlling the evolution of plastic strains. In Eq. (11),  $\bar{\boldsymbol{\sigma}}$  can be viewed as the ‘‘direction’’ of the plastic flows and  $\dot{\lambda}$  the plastic multiplier in classical plasticity.

Differentiating Eq. (9) to time and calling for Eq. (11), one obtains the rate form between the effective stress and the strain tensor as follows

$$\dot{\bar{\boldsymbol{\sigma}}} = \mathbf{S}_0 : (\dot{\boldsymbol{\varepsilon}} - \dot{\boldsymbol{\varepsilon}}^p) = \bar{\mathbf{S}}^{ep} : \dot{\boldsymbol{\varepsilon}} \quad (13)$$

where  $\bar{\mathbf{S}}^{ep}$  is the effective elastoplastic tangent tensor expressed as

$$\bar{\mathbf{S}}^{ep} = \mathbf{S}_0 - E_0[\xi^+ H(\dot{d}^+) + \xi^- H(\dot{d}^-)]H(\mathbf{l}_{\bar{\sigma}}:\dot{\boldsymbol{\varepsilon}})(\mathbf{l}_{\bar{\sigma}} \otimes \mathbf{l}_{\bar{\sigma}}) \quad (14)$$

with  $\mathbf{l}_{\bar{\sigma}} = \bar{\boldsymbol{\sigma}}/\|\bar{\boldsymbol{\sigma}}\|$  being the unit tensor of  $\bar{\boldsymbol{\sigma}}$  and  $\|\bar{\boldsymbol{\sigma}}\| = \sqrt{\bar{\boldsymbol{\sigma}}:\bar{\boldsymbol{\sigma}}}$  denoting the norm of  $\bar{\boldsymbol{\sigma}}$ .

To describe the different nonlinear behavior of concrete under tension and compression,  $\bar{\boldsymbol{\sigma}}$  and its rate tensor  $\dot{\bar{\boldsymbol{\sigma}}}$  are decomposed into their positive and negative components  $(\bar{\boldsymbol{\sigma}}^+, \bar{\boldsymbol{\sigma}}^-)$  and  $(\dot{\bar{\boldsymbol{\sigma}}}^+, \dot{\bar{\boldsymbol{\sigma}}}^-)$  as follows

$$\bar{\boldsymbol{\sigma}}^\pm = \mathbf{P}^\pm:\bar{\boldsymbol{\sigma}}; \quad \dot{\bar{\boldsymbol{\sigma}}}^\pm = \mathbf{P}^\pm:\dot{\bar{\boldsymbol{\sigma}}} \quad (15)$$

where representing the  $n^{\text{th}}$  eigenvalue and the corresponding eigenvector of  $\bar{\boldsymbol{\sigma}}$  by  $\sigma^{(n)}$  and  $\mathbf{v}^{(n)}$ , the positive and negative projection operators of  $\bar{\boldsymbol{\sigma}}$  are expressed as

$$\mathbf{P}^+ = \sum_{n=1}^3 H(\sigma^{(n)})\mathbf{V}^{(nn)} \otimes \mathbf{V}^{(nn)} + 2 \sum_{\substack{n=1 \\ m>n}}^3 \frac{\langle \sigma^{(n)} \rangle - \langle \sigma^{(m)} \rangle}{\sigma^{(n)} - \sigma^{(m)}} \mathbf{V}^{(nm)} \otimes \mathbf{V}^{(nm)}; \quad \mathbf{P}^- = \mathbf{I} - \mathbf{P}^+ \quad (16)$$

with  $\mathbf{I}$  being the fourth-order identity tensor and the second-order symmetric tensor  $\mathbf{V}^{(nm)}$  expressed as

$$\mathbf{V}^{(nm)} = \mathbf{V}^{(mn)} = \frac{1}{2}(\mathbf{v}^{(n)} \otimes \mathbf{v}^{(m)} + \mathbf{v}^{(m)} \otimes \mathbf{v}^{(n)}) \quad (17)$$

With the elastic Helmholtz free energy defined as the degradation of the initial elastic strain energy, the following constitutive relation is obtained (Wu *et al.* 2006)

$$\boldsymbol{\sigma} = (1 - d^+)\bar{\boldsymbol{\sigma}}^+ + (1 - d^-)\bar{\boldsymbol{\sigma}}^- = (\mathbf{I} - \mathbf{D}):\bar{\boldsymbol{\sigma}} \quad (18)$$

where the fourth-order symmetric tensor  $\mathbf{D}$  is the damage tensor, expressed as

$$\mathbf{D} = d^+\mathbf{P}^+ + d^-\mathbf{P}^- \quad (19)$$

**Remark 1.** The evolution rule for the plastic strains in Eqs. (11) and (12) can be viewed as an extension of an earlier proposal in Faria *et al.* (1998). However, there exist several distinct differences between the two rules: (i) Faria *et al.* assumed that the flow “direction” is elastic strain  $\boldsymbol{\varepsilon}^e$ , but here the effective stress  $\bar{\boldsymbol{\sigma}}$  is adopted since the plastic potential and the flow direction are function of  $\bar{\boldsymbol{\sigma}}$  in the effective stress space plasticity (Ju 1989, Wu *et al.* 2006); and (ii) the plastic strains under tensile stress states are prevented by the formulation in Faria *et al.*, but are accounted for in the present model.

### 2.3 CDM-based damping model

Following the basic idea presented in Section 2.1, here an effective damping stress  $\bar{\boldsymbol{\sigma}}_{\text{vis}}$  in the damaged material is defined to follow the standard visco-elastic relation

$$\bar{\boldsymbol{\sigma}}_{\text{vis}} = \beta_{\mathbf{K}}\mathbf{S}_0:\dot{\boldsymbol{\varepsilon}} \quad (20)$$

where  $\beta_{\mathbf{K}}$  is the classical Rayleigh stiffness-proportional damping parameter introduced in Eq. (1).

Similarly,  $\bar{\sigma}_{\text{vis}}$  and its rate tensor  $\dot{\bar{\sigma}}_{\text{vis}}$  can also be decomposed into their positive and negative components  $(\bar{\sigma}_{\text{vis}}^+, \bar{\sigma}_{\text{vis}}^-)$  and  $(\dot{\bar{\sigma}}_{\text{vis}}^+, \dot{\bar{\sigma}}_{\text{vis}}^-)$  as follows

$$\bar{\sigma}_{\text{vis}}^\pm = \mathbf{P}_{\text{vis}}^\pm : \bar{\sigma}_{\text{vis}}; \quad \dot{\bar{\sigma}}_{\text{vis}}^\pm = \mathbf{P}_{\text{vis}}^\pm : \dot{\bar{\sigma}}_{\text{vis}} \quad (21)$$

where  $\mathbf{P}_{\text{vis}}^\pm$  are the projection operators of  $\bar{\sigma}_{\text{vis}}$  which can be referred to Eq. (16).

Taking the tensile and shear damage mechanisms into consideration, one obtains the following expression for the Cauchy damping stress  $\sigma_{\text{vis}}$

$$\sigma_{\text{vis}} = (1 - d^+) \bar{\sigma}_{\text{vis}}^+ + (1 - d^-) \bar{\sigma}_{\text{vis}}^- = (\mathbf{I} - \mathbf{D}_{\text{vis}}) : \bar{\sigma}_{\text{vis}} \quad (22)$$

where the fourth-order symmetric tensor  $\mathbf{D}_{\text{vis}}$  is the damage tensor of the damping stress expressed as

$$\mathbf{D}_{\text{vis}} = d^+ \mathbf{P}_{\text{vis}}^+ + d^- \mathbf{P}_{\text{vis}}^- \quad (23)$$

Substituting Eqs. (18) and (22) into Eq. (8), one obtains the total stress  $\sigma_{\text{tot}}$  due to external loadings

$$\sigma_{\text{tot}} = \sigma + \sigma_{\text{vis}} = (1 - d^+) \bar{\sigma}_{\text{tot}}^+ + (1 - d^-) \bar{\sigma}_{\text{tot}}^- \quad (24)$$

where  $\bar{\sigma}_{\text{tot}}^+$  and  $\bar{\sigma}_{\text{tot}}^-$  are defined as

$$\bar{\sigma}_{\text{tot}}^+ = \bar{\sigma}^+ + \bar{\sigma}_{\text{vis}}^+; \quad \bar{\sigma}_{\text{tot}}^- = \bar{\sigma}^- + \bar{\sigma}_{\text{vis}}^- \quad (25)$$

**Remark 2.** Substituting the above defined damping stress in Eq. (22) into Eq. (6) leading to the following damping force  $\mathbf{F}^{\text{vis}}$

$$\mathbf{F}^{\text{vis}}(\mathbf{u}, \dot{\mathbf{u}}) = \beta_{\mathbf{K}} \int_{\Omega} \mathbf{B}^T [(\mathbf{I} - \mathbf{D}_{\text{vis}}) : \mathbf{S}_0 : \dot{\boldsymbol{\varepsilon}}] d\Omega = \Xi(\mathbf{u}, \dot{\mathbf{u}}) \dot{\mathbf{u}} \quad (26)$$

where the nonlinear damping matrix  $\Xi(\mathbf{u}, \dot{\mathbf{u}})$  is

$$\Xi(\mathbf{u}, \dot{\mathbf{u}}) = \beta_{\mathbf{K}} \int_{\Omega} \mathbf{B}^T [(\mathbf{I} - \mathbf{D}_{\text{vis}}) : \mathbf{S}_0] \mathbf{B} d\Omega = \beta_{\mathbf{K}}^* \mathbf{K}(\mathbf{u}, \dot{\mathbf{u}}) \quad (27)$$

with  $^* \mathbf{K}(\mathbf{u}, \dot{\mathbf{u}})$  being the damping-related stiffness matrix of the discretized structure, i.e.

$$^* \mathbf{K}(\mathbf{u}, \dot{\mathbf{u}}) = \int_{\Omega} \mathbf{B}^T [(\mathbf{I} - \mathbf{D}_{\text{vis}}) : \mathbf{S}_0] \mathbf{B} d\Omega \quad (28)$$

As long as the corresponding integration points of a finite element remain linear, i.e.  $d^+ = d^- = 0$ , Eqs. (23) and (28) lead to  $^* \mathbf{K}(\mathbf{u}, \dot{\mathbf{u}}) = \mathbf{K}_0$  where  $\mathbf{K}_0$  denotes the initial linear elastic matrix, indicating that the proposed damping model reduces to the classical Rayleigh stiffness-proportional damping one. From Eqs. (26)-(28), it can also be concluded that once the damages in the material increase, the damping force  $\mathbf{F}^{\text{vis}}$  and damping-related stiffness matrix  $^* \mathbf{K}(\mathbf{u}, \dot{\mathbf{u}})$  will decrease correspondingly. Upon crack closure the stiffness and hence the damping will be partially restored due to the unilateral effect under cyclic loadings.

The above facts agree with the observed phenomena, demonstrating the justification of the proposed damping model.

#### 2.4 Characterization of damage

In order to determine the damage states, damage criteria should be introduced analogous to the yield criteria in plasticity. In Wu *et al.* (2006), the contribution of plastic strains was considered to derive the following elastoplastic DERRs  $Y^\pm$

$$Y^+ = \sqrt{E_0(\bar{\boldsymbol{\sigma}}^+ : \mathbf{C}_0 : \bar{\boldsymbol{\sigma}}^+)}; \quad Y^- = \alpha \bar{I}_1 + \sqrt{3\bar{J}_2} \quad (29)$$

where  $\bar{I}_1$  and  $\bar{J}_2$  are the first invariant of  $\bar{\boldsymbol{\sigma}}$  and the second invariant of  $\bar{\boldsymbol{s}}$  (the deviatoric component of  $\bar{\boldsymbol{\sigma}}$ ), respectively;  $\alpha = (\vartheta - 1)/(2\vartheta - 1)$  with  $\vartheta$  being the ratio between the strengths under equibiaxial and uniaxial compression (usually in the range of 1.1~1.2) which takes the value of 1.16 in the present model leading to  $\alpha = 0.1212$ .

Therefore, thermodynamically consistent DERR-based damage criteria are established as

$$G^\pm(Y^\pm, r^\pm) = Y^\pm - r^\pm \leq 0 \quad (30)$$

with  $r^\pm$  being the current damage thresholds controlling the size of the damage surfaces. Correspondingly, the initial tensile and shear damage thresholds  $r_0^\pm$  are valuated as

$$r_0^+ = f_0^+; \quad r_0^- = (1 - \alpha)f_0^- \quad (31)$$

where  $f_0^+$  and  $f_0^-$  are the stresses (positive) beyond which nonlinearity becomes visible under uniaxial tension and uniaxial compression, respectively.

For rate-independent materials, upon damage loading the evolution laws for  $r^\pm$  can be determined by calling for the damage consistency condition, i.e.

$$\dot{G}(Y^\pm, r^\pm) = 0 \Leftrightarrow \dot{r}^\pm = \dot{Y}^\pm \quad (32)$$

For rate-dependent materials, such as concrete, the above Eq. (32) no longer holds right. Here analogous to the Perzyna-type viscoplastic regularization (Perzyna 1966), the following evolution rules for  $r^\pm$  are postulated similar to those previously proposed by others (Simo and Ju 1987, Ju 1989, Cervera *et al.* 1996, Faria *et al.* 1998)

$$\dot{r}^\pm = \mu^\pm \langle \phi^\pm(G^\pm) \rangle; \quad \phi^\pm(G^\pm) = (G^\pm/r^\pm)^{a^\pm} = (Y^\pm/r^\pm - 1)^{a^\pm} \quad (33)$$

where  $\phi^\pm$  are the viscous flow functions of the damage thresholds (Cervera *et al.* 1996);  $\mu^\pm$  are the viscous coefficients;  $a^\pm$  are positive exponents assumed to be material properties. According to the experiment data of Suraris and Shah (1984), here the following values are adopted as:  $\mu^+ = 2.1 \times 10^{10}$  N/s.m,  $\mu^- = 6.0 \times 10^{11}$  N/s.m,  $a^+ = 5.5$  and  $a^- = 4.5$ .

Applying the normality rule to the damage criteria expressed in Eq. (30) and performing a trivial integration, one obtains (Faria *et al.* 1998, Wu *et al.* 2006)

$$\dot{d}^\pm = \dot{g}^\pm(r^\pm) \Leftrightarrow d^\pm = g^\pm(r^\pm) \quad (34)$$

with the following monotonically increasing functions  $g^\pm$  adopted in the present model

$$d^+ = g^+(r^+) = 1 - \frac{r_0^+}{r^+} \left\{ (1 - A^+) + A^+ \exp \left[ B^+ \left( 1 - \frac{r^+}{r_0^+} \right) \right] \right\} \quad (35)$$

$$d^- = g^-(r^-) = 1 - \left\{ \frac{r_0^-}{r^-} (1 - A^-) + A^- \exp \left[ B^- \left( 1 - \frac{r^-}{r_0^-} \right) \right] \right\} \quad (36)$$

In Eq. (35), for reinforced concrete parameters  $A^+$  and  $B^+$  should be related to the reinforcement ratio  $\rho_s$  as follows (Wu *et al.* 2006)

$$A^+ = 1 - c_s \rho_s / d_b; \quad B^+ = (270 / \sqrt{1 - A^+}) f_0^+ / E_0 \leq 1000 f_0^+ / E_0 \quad (37)$$

with  $d_b$  being the rebar diameter (in mm) and  $c_s$  generally taking the value of 75 mm. And by imposing the simulation curve to fit the one obtained from a 1D experimental test (See the Appendix for details), parameters  $A^-$  and  $B^-$  in Eq. (36) may be determined as

$$A^- = \frac{1 - d_p^- - B^-}{\exp(B^- - 1) - B^-}; \quad B^- = (1 - d_p^-) f_0^- / f_c \quad (38)$$

where  $f_0^-$  and  $f_c$  respectively denotes the linear-elastic strength and the peak strength under uniaxial compression;  $d_p^-$  denotes the shear damage up to  $f_c$ , which can be determined by measuring the degradation of unloading stiffness.

### 2.5 Considerations in the plain concrete structure

It is now well known that, the softening behavior occurs on the material scale often introduces mesh sensitivity in the results obtained by the standard finite element method, in the sense that the predictions do not converge to a unique solution but leads to narrower crack bands as the mesh is refined. In practical simulations for reinforced concrete structures, the mesh is usually such that each element contains rebars. The interaction between the rebars and the concrete tends to reduce the mesh sensitivity, provided that a reasonable amount of tension stiffening is introduced in the concrete model to simulate this interaction.

However in the cases with little or no reinforcement, e.g., the plain concrete, rock, etc., when the tangent stiffness no longer remains positive definite, the parameters  $A^+$  and  $B^+$  expressed in Eq. (37) are inappropriate to model those materials with strain softening regions unless the model is non-locally regularized. To circumscribe the spurious mesh sensitivity, many methods have been proposed in the literature among which the most popular are the non-local methods (Pijaudier-Cabot and Bazant 1988, Bazant and Pijaudier-Cabot 1989, etc.), the gradient models (de Borst *et al.* 1995, Peerlings *et al.* 1996, Comi 1998, etc.), the strong (weak) discontinuity models (Belytschko *et al.* 1988, Oliver and Simo 1994, Oliver 1996, Ortiz *et al.* 1987, Simo 1993, etc.) and the imbedded cracks methods (Jirasek and Zimmermann 2001). However, all the numerical implementations of the above methods either lead to complex algorithm or require enhancements of the standard finite element method. And more importantly, the dynamic nonlinear analysis of massive concrete structure is greatly time-consuming, and is worsened if the full Newton-Raphson algorithm is adopted. The above facts make them impractical in the actual engineering concrete structures.

Here the concept of crack bank theory (Bazant and Oh 1983, Rots 1988, Mang and Hofsetter

1995, Calayir and Karson 2005, etc.) is employed. Under such conditions, Eq. (37) renders  $A^+ = 1.0$ , and therefore Eq. (35) reduces to the following simple one-parameter function

$$d^+ = g^+(r^+) = 1 - \frac{r_0^+}{r^+} \exp \left[ B^+ \left( 1 - \frac{r^+}{r_0^+} \right) \right] \quad (39)$$

where for plain concrete, the value of  $B^+$  are no longer constant, but is dependent on the mesh sizes and related to  $G_f^+/l_{ch}$ , with  $G_f^+$  signifying the Mode-I fracture energy assumed as material properties, and  $l_{ch}$  denoting the characteristic length of the finite element meshes. Applying Eq. (39) to uniaxial tension and integrating the area under the obtained stress-strain curve, one obtains

$$\frac{G_f^+}{l_{ch}} = \int_0^\infty (1 - d^+) E_0 \varepsilon d\varepsilon \Rightarrow B^+ = \left( \frac{G_f^+ E_0}{l_{ch} (f_0^+)^2} - \frac{1}{2} \right)^{-1} \quad (40)$$

Based on the method originated by Oliver *et al.* (1990), the following measure of the characteristic length is approximated as  $l_{ch} = n_{\text{dim}} \sqrt{V}$  ( $n_{\text{dim}} = 1, 2, 3$ ), with  $V$  and  $n_{\text{dim}}$  denoting the volume and the spatial dimension of the elements, respectively. As stated in Scotta *et al.* (2001), the adopted expression for characteristic length can ensure sufficient preciseness independent the mesh sizes, comparing to the analytical values in concern to the energy dissipation. Though the parameters determined from the crack band theory can not completely eliminate the dependence of the numerical solution on the mesh refinement, the critical advantage over other methods is obvious: It requires an ignorable increase of the consuming time, and can be directly implemented into the standard finite element programs. It is noted that, if the softening behavior under compression is of great significance to the analysis, the above crack-band method can also be similarly employed to minimize the mesh-dependence.

The concerned computation aspects are to be discussed in the next section.

### 3. Computational aspects

#### 3.1 Linearization of governing equation of motion

In accordance with the HHT- $\alpha$  method (Hughes 1987), at current increment step  $n+1$  the discretized form of the equation of motion in Eq. (4) is written as

$$\mathbf{M} \ddot{\mathbf{u}}_{n+1} + \mathbf{F}_{n+1-\alpha_f} = \mathbf{F}_{n+1-\alpha_f}^{\text{ext}} \quad (41)$$

or its linearization form

$$\left[ \mathbf{M} \frac{d\ddot{\mathbf{u}}_{n+1}}{d\mathbf{u}_{n+1}} + (1 - \alpha_f) \frac{d\mathbf{F}_{n+1}}{d\mathbf{u}_{n+1}} \right] \Delta \mathbf{u} = (1 - \alpha_f) \Delta \mathbf{F}^{\text{ext}} \quad (42)$$

with  $\Delta \mathbf{u}$  and  $\Delta \mathbf{F}^{\text{ext}}$  being the displacement and the external load increment vectors, respectively, and  $\mathbf{F}_{n+1-\alpha_f}$  expressed as

$$\mathbf{F}_{n+1-\alpha_f} = \alpha_f \mathbf{F}_n + (1 - \alpha_f) \mathbf{F}_{n+1} = \alpha_f \mathbf{F}_n + (1 - \alpha_f) \int_{\Omega} \mathbf{B}^T (\boldsymbol{\sigma}_{\text{tot}})_{n+1} d\Omega \quad (43)$$

where parameter  $\alpha_f$  is to reduce the high-frequency numerical noise and  $0 \leq \alpha_f \leq 1/3$  leads to the unconditional stability of the above integration method. In the present model,  $\alpha_f = 0.05$  is adopted to quickly remove the high frequency noise without any significant effect on the meaningful lower frequency response (the numerical dissipation is always quite small, mostly less than 1% of the total energy).

The linear acceleration field assumption of Newmark- $\beta$  method yields the following expressions for the velocity and acceleration increment vectors

$$\Delta \dot{\mathbf{u}}_{n+1} = \frac{\gamma}{\beta_f \Delta t} \Delta \mathbf{u}_{n+1} + \left(1 - \frac{\gamma}{2\beta_f}\right) \Delta \dot{\mathbf{u}}_n - \frac{\gamma}{\beta_f} \dot{\mathbf{u}}_n \quad (44)$$

$$\Delta \ddot{\mathbf{u}}_{n+1} = \frac{1}{\beta_f \Delta t^2} \Delta \mathbf{u}_{n+1} - \frac{1}{\beta_f \Delta t^2} \left( \dot{\mathbf{u}}_n \Delta t + \frac{1}{2} \ddot{\mathbf{u}}_n \Delta t^2 \right) \quad (45)$$

where  $\Delta t$  is the increment of time;  $\beta_f$  and  $\gamma$  are parameters related to  $\alpha_f$

$$\beta_f = \frac{1}{4}(1 + \alpha_f)^2; \quad \gamma = \frac{1}{2} + \alpha_f \quad (46)$$

Correspondingly, from Eq. (44) the strain rate  $\dot{\boldsymbol{\varepsilon}}_{n+1}$  in Eq. (20) becomes

$$\dot{\boldsymbol{\varepsilon}}_{n+1} = \frac{\gamma}{\beta_f \Delta t} \Delta \boldsymbol{\varepsilon} \quad (47)$$

where  $\Delta \boldsymbol{\varepsilon}$  denotes the increment of  $\boldsymbol{\varepsilon}$ . Substituting Eqs. (44) and (45) into Eq. (42) and after some simple mathematics manipulations, one obtains the quasi-static governing equation in an increment format

$$\bar{\mathbf{K}}^{\text{tan}} \Delta \mathbf{u} = \Delta \mathbf{P} \quad (48)$$

where  $\Delta \mathbf{P}$  is the increment of the quasi-static external loading vector, and the quasi-static tangent matrix  $\bar{\mathbf{K}}^{\text{tan}}$  is expressed as

$$\bar{\mathbf{K}}^{\text{tan}} = \frac{1}{\beta_f (\Delta t)^2} \mathbf{M} + (1 - \alpha_f) \int_{\Omega} \mathbf{B}^T \left( \frac{d\boldsymbol{\sigma}_{\text{tot}}}{d\boldsymbol{\varepsilon}} \right)_{n+1} \mathbf{B} d\Omega \quad (49)$$

It can be clearly seen from Eqs. (43) and (49), the numerical implementation of the proposed unified plastic-damage model requires to carry out two main tasks: (i) updating the total stress  $(\boldsymbol{\sigma}_{\text{tot}})_{n+1}$  with a stable algorithm; (ii) providing the corresponding algorithmic consistent modulus  $(d\boldsymbol{\sigma}_{\text{tot}}/d\boldsymbol{\varepsilon})_{n+1}$  (Simo and Hughes 1998). Once the above jobs are completed, the dynamic nonlinear analysis of damping structures can be transformed into the conventional quasi-static one to be solved by the general finite element method (Zienkiewicz and Taylor 2000).

### 3.2 Stress updating algorithm

From Eq. (47)  $\dot{\boldsymbol{\varepsilon}}_{n+1}$  is explicit and the effective damping stress  $(\bar{\boldsymbol{\sigma}}_{\text{vis}})_{n+1}$  can thus be directly computed through Eq. (20), so only the effective stress  $\bar{\boldsymbol{\sigma}}_{n+1}$  is required to update the total stress  $(\boldsymbol{\sigma}_{\text{tot}})_{n+1}$ . For the proposed evolution law for the plastic strain, the backward-Euler time discretization method is applied to integrate Eq. (13), leading to

$$\bar{\sigma}_{n+1} = \bar{\sigma}_n + \mathbf{S}_0 : \Delta \boldsymbol{\varepsilon} + E_0 [\xi^+ H(\dot{d}_{n+1}^+) + \xi^- H(\dot{d}_{n+1}^-)] \langle \mathbf{I}_{\bar{\sigma}_{n+1}} : \Delta \boldsymbol{\varepsilon} \rangle \mathbf{I}_{\bar{\sigma}_{n+1}} \quad (50)$$

Introducing

$$\bar{\sigma}_{n+1}^{\text{trial}} = \bar{\sigma}_n + \mathbf{S}_0 : \Delta \boldsymbol{\varepsilon} \quad (51)$$

Similar to the method proposed in Faria *et al.* (1998), the following relation is then obtained to update  $\bar{\sigma}_{n+1}$

$$\bar{\sigma}_{n+1} = \eta_{n+1} \bar{\sigma}_{n+1}^{\text{trial}} \quad (52)$$

where

$$\eta_{n+1} = 1 - E_0 [\xi^+ H(\dot{d}_{n+1}^+) + \xi^- H(\dot{d}_{n+1}^-)] \frac{\langle \mathbf{I}_{\bar{\sigma}_{n+1}^{\text{trial}}} : \Delta \boldsymbol{\varepsilon} \rangle}{\|\bar{\sigma}_{n+1}^{\text{trial}}\|} \quad (53)$$

It can be seen that in Eqs. (51) and (52)  $\bar{\sigma}_{n+1}$  can be updated analogous to the classical radial returning mapping algorithm which includes the elastic-predictor and plastic-corrector steps: since  $\Delta \boldsymbol{\varepsilon}$  is provided in a strain-based algorithm, the elastic-predictor  $\bar{\sigma}_{n+1}^{\text{trial}}$  is calculated by Eq. (51) and then  $\bar{\sigma}_{n+1}$  can be updated by Eq. (52). High numerical efficiency can be thus guaranteed by the proposed evolution law for the plastic strain, since a maximum of four iterations are required due to the 0/1 discontinuity resulted from the Heaviside function.

Once  $\bar{\sigma}_{n+1}$  is obtained and then decomposed into its positive and negative components ( $\bar{\sigma}_{n+1}^+$ ,  $\bar{\sigma}_{n+1}^-$ ), by Eqs. (29) the DERRs  $Y_{n+1}^\pm$  can thus be valued to update  $r_{n+1}^\pm$  as follows.

For rate-independent cases, integrating Eq (32) under given initial conditions, one obtains the updated values of  $r_{n+1}^\pm$  as

$$r_{n+1}^\pm = \max \left\{ r_0^\pm, \max_{\tau \in [0, t]} (Y_\tau^\pm) \right\} \quad (54)$$

For rate-dependent cases, with the unconditionally stable trapezoidal method, the updated  $r_{n+1}^\pm$  can be written as the following residual form

$$f(r_{n+1}^\pm) = -r_{n+1}^\pm + r_n^\pm + \Delta t \mu^\pm \langle Y_{n+1/2}^\pm / r_{n+1/2}^\pm - 1 \rangle^{a^\pm} = 0 \quad (55)$$

where

$$Y_{n+1/2}^\pm = (Y_{n+1}^\pm + Y_n^\pm)/2; \quad r_{n+1/2}^\pm = (r_{n+1}^\pm + r_n^\pm)/2 \quad (56)$$

Since the value of  $a^\pm \neq 1$  is adopted in the present model, Eq. (55) is the nonlinear function of  $r_{n+1}^\pm$ , which can be solved by the Newton-Raphson algorithm whose iteration form is

$${}^{(k+1)}r_{n+1}^\pm = {}^{(k)}r_{n+1}^\pm - f(r_{n+1}^\pm) / f'(r_{n+1}^\pm) \quad (57)$$

where  ${}^{(k+1)}(\cdot)$  denotes the improved entity after  $(k+1)$ th iteration and  $f'(r_{n+1}^\pm)$  is the derivative of  $f(r_{n+1}^\pm)$  to  $r_{n+1}^\pm$ , expressed as

$$f'(r_{n+1}^\pm) = -1 - 0.5 \Delta t a^\pm \mu^\pm Y_{n+1/2}^\pm \langle Y_{n+1/2}^\pm / r_{n+1/2}^\pm - 1 \rangle^{a^\pm - 1} / (r_{n+1/2}^\pm)^2 \quad (58)$$

After  $r_{n+1}^{\pm}$  are updated through Eq. (54) or Eqs. (55)-(58), the damage variables  $d_{n+1}^{\pm}$  can be calculated by Eqs. (35) and (36) and the total stress  $(\boldsymbol{\sigma}_{\text{tot}})_{n+1}$  can be updated by Eq. (24).

### 3.3 Consistent tangent moduli

Taking derivative of Eqs. (50) and (20) and calling for Eqs. (53) and (47), one obtains

$$\frac{d\bar{\boldsymbol{\sigma}}}{d\boldsymbol{\varepsilon}} = \bar{\mathbf{S}}^{\text{alg}}; \quad \frac{d\bar{\boldsymbol{\sigma}}_{\text{vis}}}{d\boldsymbol{\varepsilon}} = \bar{\mathbf{S}}_{\text{vis}}^{\text{alg}} \quad (59)$$

where the subscript  $n+1$  is omitted in this section for expression simplicity; the fourth-order tensor  $\bar{\mathbf{S}}^{\text{alg}}$  and  $\bar{\mathbf{S}}_{\text{vis}}^{\text{alg}}$  are the consistent effective tangent modulus due to the deformations and damping, respectively, expressed as

$$\bar{\mathbf{S}}^{\text{alg}} = \mathbf{S}_0 - \frac{(1-\eta)}{\bar{\boldsymbol{\sigma}}^{\text{trial}} : \Delta \boldsymbol{\varepsilon}} (\bar{\boldsymbol{\sigma}}^{\text{trial}} \otimes \bar{\boldsymbol{\sigma}}^{\text{trial}}); \quad \bar{\mathbf{S}}_{\text{vis}}^{\text{alg}} = \frac{\beta_{\mathbf{k}} \gamma_f}{\beta_f \Delta t} \mathbf{S}_0 \quad (60)$$

With the above results, the derivatives of the Cauchy stress in Eq. (18) and the damping stress in Eq. (22) can be written as

$$\frac{d\boldsymbol{\sigma}}{d\boldsymbol{\varepsilon}} = (\mathbf{I} - \mathbf{D}) : \bar{\mathbf{S}}^{\text{alg}} - \left[ \bar{\boldsymbol{\sigma}}^+ \frac{d(d^+)}{d\boldsymbol{\varepsilon}} + \bar{\boldsymbol{\sigma}}^- \frac{d(d^-)}{d\boldsymbol{\varepsilon}} \right] \quad (61)$$

$$\frac{d\boldsymbol{\sigma}_{\text{vis}}}{d\boldsymbol{\varepsilon}} = (\mathbf{I} - \mathbf{D}_{\text{vis}}) : \bar{\mathbf{S}}_{\text{vis}}^{\text{alg}} - \left[ \bar{\boldsymbol{\sigma}}_{\text{vis}}^+ \frac{d(d^+)}{d\boldsymbol{\varepsilon}} + \bar{\boldsymbol{\sigma}}_{\text{vis}}^- \frac{d(d^-)}{d\boldsymbol{\varepsilon}} \right] \quad (62)$$

For rate-dependent cases, the algorithm of updating the damage thresholds  $r^{\pm}$  given in Eq. (55) leads to

$$dr^{\pm} = \lambda_r^{\pm} dY^{\pm} \quad (63)$$

with  $\lambda_r^{\pm}$  being

$$\lambda_r^{\pm} = \frac{\Delta t \mu^{\pm} a^{\pm} r_{n+1/2}^{\pm} \langle Y_{n+1/2}^{\pm} / r_{n+1/2}^{\pm} - 1 \rangle^{a^{\pm}-1}}{2(r_{n+1/2}^{\pm})^2 + \Delta t \mu^{\pm} a^{\pm} Y_{n+1/2}^{\pm} \langle Y_{n+1/2}^{\pm} / r_{n+1/2}^{\pm} - 1 \rangle^{a^{\pm}-1}} \quad (64)$$

It can be concluded that when  $\mu^{\pm}$  approach to infinity,  $\lambda_r^{\pm}$  will tend to identity and Eq. (63) reduces to Eq. (32), demonstrating Eq. (63) applies for both the rate-independent and the rate-dependent cases. In Eq. (63)  $dY^{\pm}$  can be derived through their definitions in Eq. (29)

$$dY^+ = \frac{E_0}{2Y^+} (\bar{\boldsymbol{\sigma}} : \mathbf{C}_0 : \mathbf{P}^+ + \bar{\boldsymbol{\sigma}}^+ : \mathbf{C}_0) : d\bar{\boldsymbol{\sigma}} \quad (65)$$

$$dY^- = (\alpha \mathbf{I} + \sqrt{3} \bar{\mathbf{s}} / 2) : d\bar{\boldsymbol{\sigma}} \quad (66)$$

Then the derivatives in Eqs. (61) and (62) can be expressed as

$$\frac{d(d^{\pm})}{d\boldsymbol{\varepsilon}} = h^{\pm} \frac{dr^{\pm}}{d\boldsymbol{\varepsilon}} = h^{\pm} \lambda_r^{\pm} \frac{dY^{\pm}}{d\boldsymbol{\varepsilon}} \quad (67)$$

where  $h^{\pm}$  are the hardening/softening functions obtained from Eqs. (35) and (36) as follows

$$h^+ = \frac{\partial d^+}{\partial r^+} = \frac{(1-A^+)r_0^+}{(r^+)^2} + A^+ \frac{B^+ r^+ + r_0^+}{(r^+)^2} \exp \left[ B^+ \left( 1 - \frac{r^+}{r_0^+} \right) \right] \quad (68)$$

$$h^- = \frac{\partial d^-}{\partial r^-} = \frac{(1-A^-)r_0^-}{(r^-)^2} + \frac{A^- B^-}{r_0^-} \exp \left[ B^- \left( 1 - \frac{r^-}{r_0^-} \right) \right] \quad (69)$$

It is therefore possible to obtain the following relations

$$\bar{\boldsymbol{\sigma}}_{\text{tot}} \frac{d(d^\pm)}{d\boldsymbol{\varepsilon}} = \mathbf{R}_{\text{tot}}^\pm \cdot \bar{\mathbf{S}}^{\text{alg}} \quad (70)$$

with the fourth-order tensor  $\mathbf{R}_{\text{tot}}^+$  and  $\mathbf{R}_{\text{tot}}^-$  being

$$\mathbf{R}_{\text{tot}}^+ = \frac{h^+ \lambda_r^+ E_0}{2Y^+} [\bar{\boldsymbol{\sigma}}_{\text{tot}}^+ \otimes (\bar{\boldsymbol{\sigma}} : \mathbf{C}_0 : \mathbf{P}^+ + \bar{\boldsymbol{\sigma}}^+ : \mathbf{C}_0)] \quad (71)$$

$$\mathbf{R}_{\text{tot}}^- = h^- \lambda_r^- [\bar{\boldsymbol{\sigma}}_{\text{tot}}^- \otimes (\alpha \mathbf{1} + \sqrt{3} \bar{\mathbf{s}}/2)] \quad (72)$$

Calling for the definition of total stress  $\boldsymbol{\sigma}_{\text{tot}}$  in Eq. (24), the final expression for the numerical consistent tangent modulus in Eq. (49) is thus obtained as

$$\frac{d\boldsymbol{\sigma}_{\text{tot}}}{d\boldsymbol{\varepsilon}} = \frac{d\boldsymbol{\sigma}}{d\boldsymbol{\varepsilon}} + \frac{d\boldsymbol{\sigma}_{\text{vis}}}{d\boldsymbol{\varepsilon}} = (\mathbf{I} - \mathbf{D} - \mathbf{R}_{\text{tot}}) : \bar{\mathbf{S}}^{\text{alg}} + (\mathbf{I} - \mathbf{D}_{\text{vis}}) : \bar{\mathbf{S}}_{\text{vis}}^{\text{alg}} \quad (73)$$

where  $\mathbf{R}_{\text{tot}} = \mathbf{R}_{\text{tot}}^+ + \mathbf{R}_{\text{tot}}^-$  is unsymmetric fourth-order tensor.

## 4. Validation examples

In this section several examples of concrete specimens are utilized to illustrate the validity of the proposed unified plastic-damage model and the capability of reproducing the typical nonlinear behavior of concrete under static and different rate straining loading conditions, where one four-node plane stress element with characteristic length  $l_{ch} = 0.10$  m is adopted in all of the simulations.

### 4.1 Rate-independent cases

#### 4.1.1 Monotonic uniaxial tests

The experimental results from a monotonic uniaxial tensile test (Zhang 2001) and a monotonic uniaxial compression one (Karson and Jirsa 1969) are taken as the first example to check the adequacy of the numerical model. The material properties used in the simulations were: for the tensile test,  $E_0 = 38$  GPa,  $\nu_0 = 0.2$ ,  $f_0^+ = 3.4$  MPa,  $A^+ = 1.0$ ,  $G_f = 70$  N/m; and for the compressive one,  $E_0 = 31.7$  GPa,  $\nu_0 = 0.2$ ,  $f_0^- = 10.2$  MPa,  $A^- = 1.0$ ,  $B^- = 0.16$ . Fig. 1 compares the predicted stress-strain numerical curves with those obtained from the experimental tests. For both tests predictions from the present model agree well with the experimental results, either in the hardening or in the softening branches.

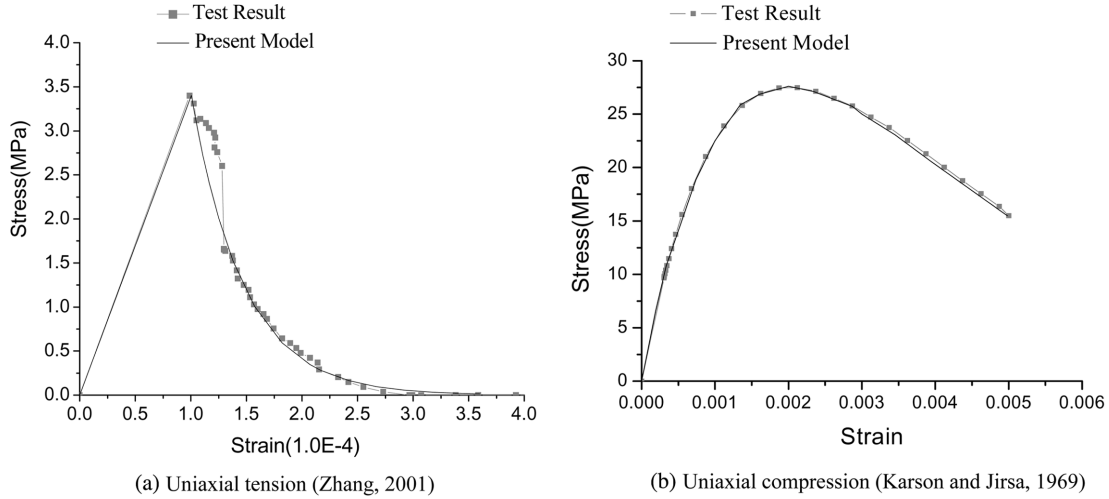


Fig. 1 Monotonic uniaxial tests

4.1.2 Monotonic biaxial tests

The proposed model is also validated with the results under biaxial compression ( $\sigma_3 = 0$ ) reported in Kupfer *et al.* (1969). The material properties adopted in the simulation were:  $E_0 = 31$  GPa,  $\nu_0 = 0.2$ ,  $f_0^+ = 3.0$  MPa,  $f_0^- = 15.0$  MPa,  $A^\pm = 1.0$ ,  $G_f = 100$  N/m,  $B^- = 0.213$ . For specimens under load conditions  $\sigma_2/\sigma_1 = -1/0$ ,  $\sigma_2/\sigma_1 = -1/-1$  and  $\sigma_2/\sigma_1 = -1/-0.52$ , the predicted stress-strain curves illustrated in Fig. 2(a) agree well with the experimental ones, capturing the overall experimental behavior.

To illustrate the capability of the proposed model for predicting the nonlinear behavior of concrete under other biaxial stress states, using the same material properties as above, the numerical biaxial strength envelope is reproduced in Fig. 2(b), almost coincident with the experimental one from Kupfer *et al.* (1969). As clearly perceptible in Fig. 2(b), another important attribute of the present

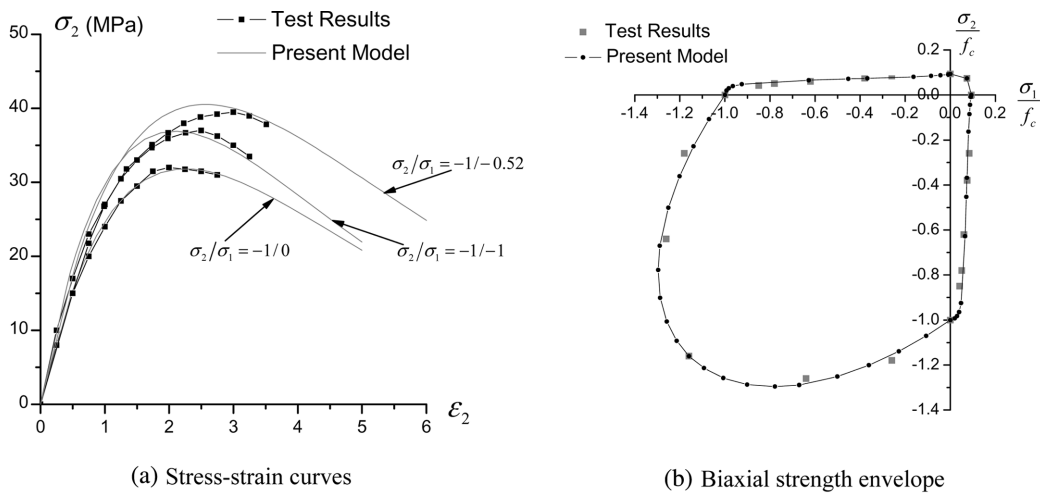
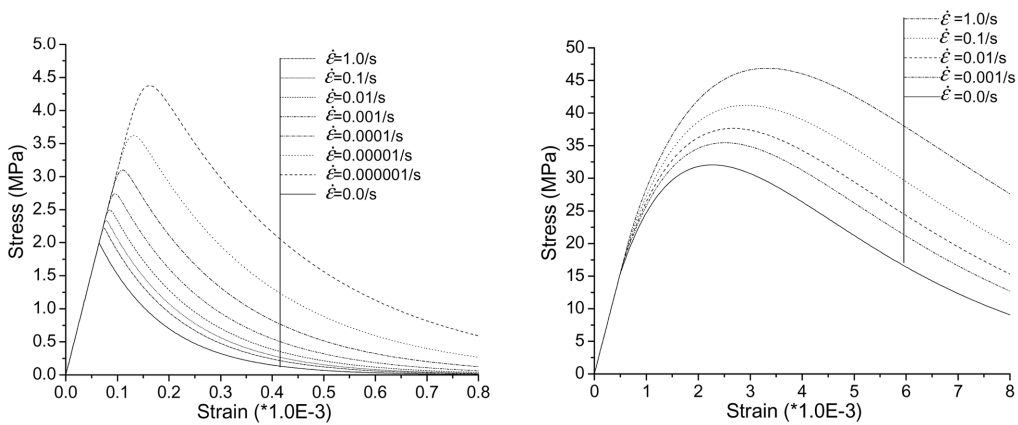


Fig. 2 Monotonic biaxial compression tests (Kupfer *et al.* 1969)

model is its ability to predict not only the strength enhancement of concrete under biaxial compression, but also the decay of the compressive strength induced by orthogonal tensile cracking under tension-compression stress states.

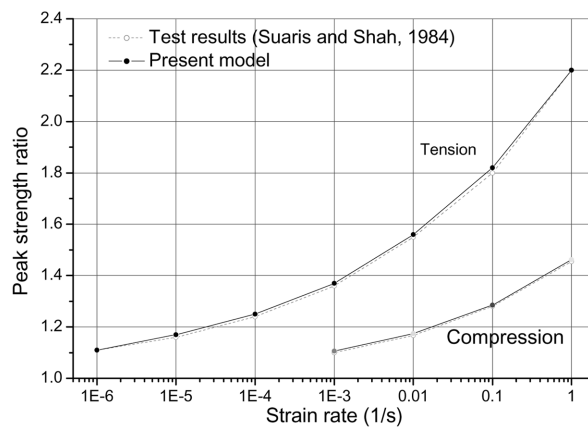
4.1.3 Rate-dependent simulations

A model concrete with the material properties of  $E_0 = 31$  GPa,  $\nu_0 = 0.2$ ,  $f_0^+ = 2.0$  MPa,  $f_0^- = 15.0$  MPa,  $A^\pm = 1.0$ ,  $G_f = 70$  N/m,  $B^- = 0.213$ , is analyzed in uniaxial tension and uniaxial compression under different strain rate  $\dot{\epsilon}$  (between  $10^{-7}/s$  and  $1/s$ ). The obtained strain-stress curves are depicted in Fig. 3(a) and Fig. 3(b) together with that of rate-independent result ( $\dot{\epsilon} = 0/s$ ). The predicted peak strength ratio versus the strain rate curves from the proposed model (see Fig. 3(c)) agree well with those obtained by Suaris and Shah (1984), illustrating the capability of the proposed model for reproducing the strain rate effect. It can be seen from Fig. 3 that under both tension and compression, (i) as the strain rate increases, the peak strength also enhances especially more pronounced in tension, which is evidenced by experimental observations (Suaris and Shah 1984);



(a) Tensile strain-rate effect

(b) Compressive strain-rate effect



(c) Peak strength ratio

Fig. 3 Strain rate effect of concrete

(ii) as the strain rate approaches to zero, the results tend to the one by the rate-independent version.

More application examples of the concrete specimens and structures under static loading can be found in Wu *et al.* (2006).

## 5. Application to Koyna dam

To further illustrate the capability of the proposed unified plastic-damage model for the dynamic nonlinear analysis of concrete structures, the Koyna dam subjected to earthquake motions in 1967, which has been extensively studied by other investigators (Chopra and Chakrabarti 1973, Bhattacharjee and Léger 1993, Ghrib and Tinawi 1995, Cervera *et al.* 1996, and Lee and Fenves 1998, etc.), is selected to be analyzed in this section.

### 5.1 Finite element modelling

The geometry of a typical non-overflow monolith of the Koyna dam which is 103 m high and 71 m wide at its base, is illustrated in Fig. 4(a). The upstream wall of the monolith is assumed to be straight and vertical, slightly different from the real configuration. The depth of the reservoir at the time of the earthquake is 91.75 m. The mechanical properties of the concrete are: density  $\rho_0 = 2643 \text{ kg/m}^3$ ,  $E_0 = 31 \text{ GPa}$ ,  $\nu_0 = 0.2$ ,  $f_c = 24.1 \text{ MPa}$ , which are taken from those used by previous investigators.

Following the work of other investigators, in this simulation the two-dimensional analysis assuming plane stress conditions is used, and two employed meshing techniques are shown in Figs. 4(b) and 4(c), where Mesh A: relative coarse meshes with seeds bias towards the slope changes on the downstream face, consists of 760 four-node plane stress quadrilateral isoperimetric elements with reduced integration, and Mesh B: uniformly distributed meshes with 1740 same type of elements. In both analyses, The dam-foundation interactions are ignored by assuming that the foundation is rigid and the hydrodynamic pressure resulted from the vertical component of the

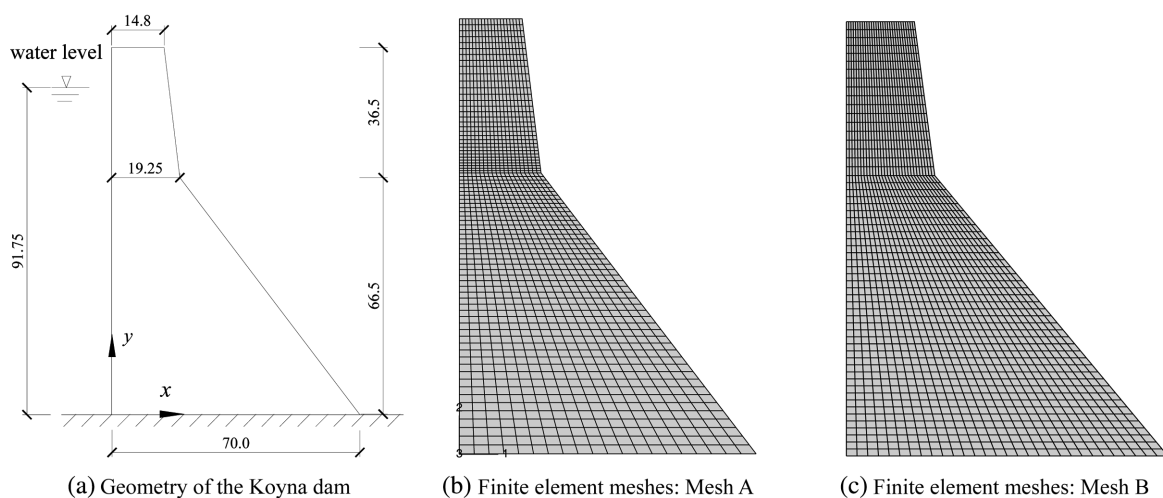


Fig. 4 Geometry and FEM meshes of Koyna dam

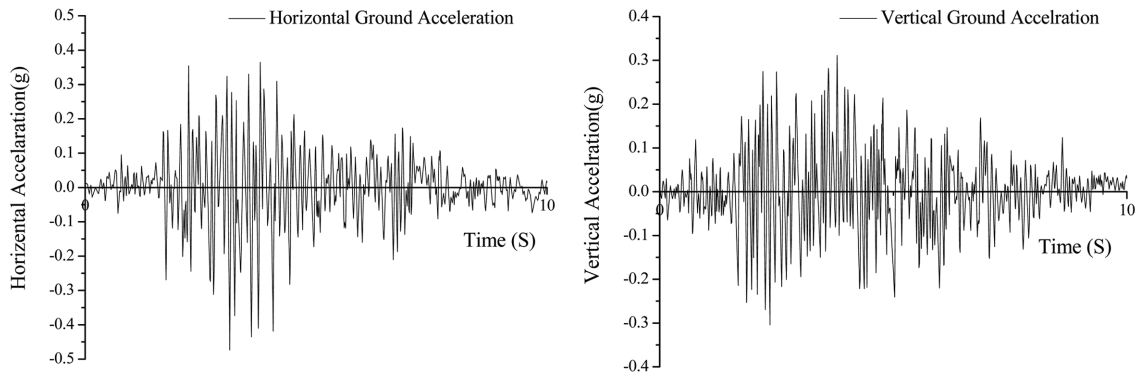
ground motion is assumed to be small enough to be neglected. The dam-reservoir interaction due to the transverse component is modeled using a 2-node element by the added mass technique (Westergaard 1933), in which the added mass per unit area of the upstream wall is given in an approximate form by the expression

$$m_w = \frac{7}{8} \rho_w \sqrt{h_w (h_w - y)} \quad (y \leq h_w) \tag{74}$$

where  $\rho_w = 1000 \text{ kg/m}^3$  and  $h_w$  are the water density and the height relative to the foundation.

The transverse and vertical components of the ground accelerations recorded during the Koyna earthquake are shown in Fig. 5 (units of  $g = 9.81 \text{ m/sec}^2$ ). In the first step, a static analysis for the dam is carried out to the gravity loading and to the hydrostatic pressure of the reservoir on the upstream wall. A frequency extraction analysis without the reservoir is then performed to determine the first four natural frequencies as shown in Table 1, which are in good agreement with the values reported by Chopra and Chakrabarti (1973). The material damping property is assumed to provide a 3% (between the general accepted about 2-5%) fraction of the critical damping for the first mode of vibration of the dam, and then from Eq. (2) with  $\beta_M = 0$  and  $\omega_1 = 18.87 \text{ rad/s}$ , one obtains  $\beta_K = 0.003183s$ .

The other model parameters adopted for the simulation are:  $f_0^+ = f_i = 0.1f_c = 2.41 \text{ MPa}$ ,  $f_0^- = 10.0 \text{ MPa}$ ,  $A^\pm = 1.0$ ,  $G_f = 200 \text{ N/m}$ ,  $B^- = 0.18$ ,  $\xi^+ = 0.10$ ,  $\xi^- = 0.20$ . It is noted that here no empirical enhancement of the tensile strength  $f_i$  is made as in Lee and Fenves (1998) since the strain rate effect can be well captured by the presented unified model.



(a) Transverse component

(b) Vertical component

Fig. 5 Ground accelerations of Koyna earthquake

Table 1 Natural frequencies of the Koyna dam

Mode No.	Natural frequency (rad/s)	
	Present model	Chopra and Chakrabarti (1973)
1	18.87	19.27
2	50.11	51.50
3	68.18	67.56
4	98.77	99.73

## 5.2 Results of dynamic nonlinear analysis

With the above parameters, the nonlinear responses of the dam under the horizontal and vertical earthquake excitations are then analyzed.

Firstly, the nonlinear and linear analyses with Mesh A are carried on and the numerical predictions are showed in Fig. 6(a), represented with the time-history of the relative spatial horizontal displacement (to the ground motion) at the left corner of the crest (the positive values represent the displacement in the downstream direction). The predicted results show the necessity of considering the nonlinear behavior of concrete, since the linear analysis greatly overestimates the response of concrete structures.

Secondly, two nonlinear analyses are carried on adopting the two finite element meshes. The reproduced results of the relative horizontal displacement at the left corner of the crest, are shown in Fig. 6(b). Noted that the obtained two time-history curves are rather close to each other, demonstrating the effectiveness of adopted crack band theory in guaranteeing the mesh objectivity in the sense of structural responses.

From Fig. 6(b), it can also be seen the crest displacement remains less than 30 mm during the first 4 seconds of the earthquake, and after these 4 seconds, the amplitude of the oscillation of the crest increases substantially, demonstrating severe damage evolved in the structure during these oscillations.

The predicted evolution of tensile damage with Mesh A in the concrete dam at six different times during the earthquake is illustrated in Fig. 7. Times  $t_1=3.958s$ ,  $t_3=4.363s$ , and  $t_5=4.747s$  correspond to the first three large excursions of the crest in the upstream direction, and times  $t_2=4.165s$  and  $t_4=4.534s$  correspond to the first two large excursions of the crest in the downstream direction. And time  $t_6=10.000s$  corresponds to the end of the earthquake excitation.

As another statement that the presented analysis is also mesh-independence controlled in the sense of local responses, the distributions of tensile damage in the dam at the last analysis time  $t_6$  are compared in Fig. 8 for two finite meshes. It can be clearly seen that damage has evolved at the base of the dam on the upstream face due to the infinitely rigid foundation and in the region near the stress concentration where the slope on the downstream face changes. Also tensile damage

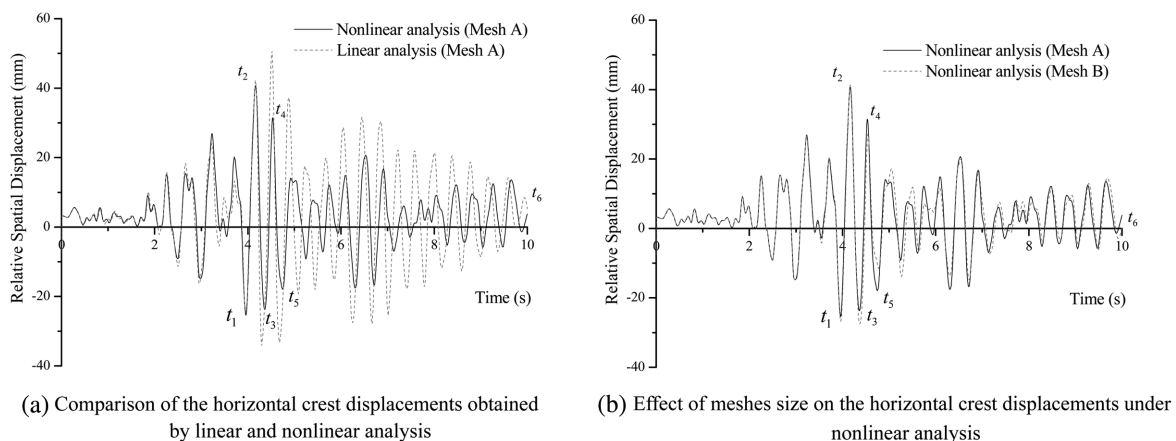


Fig. 6 Predicted results of Koyna dam

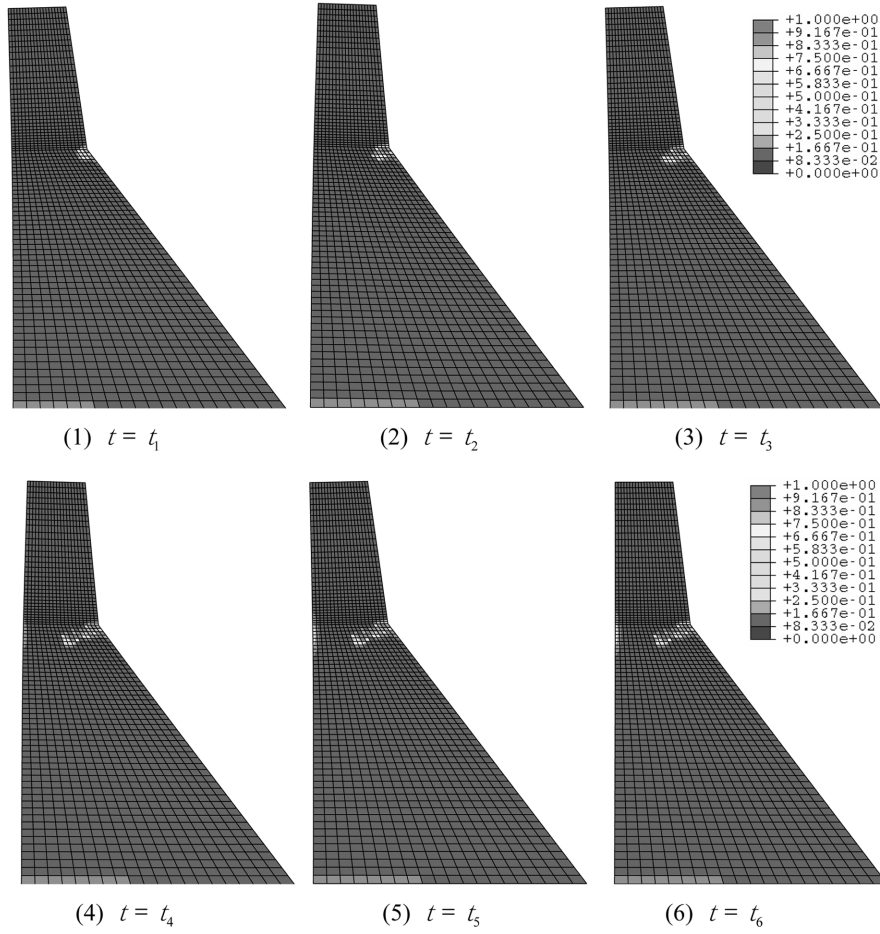


Fig. 7 Evolution of tensile damage (Mesh A of deformation scale factor = 50)

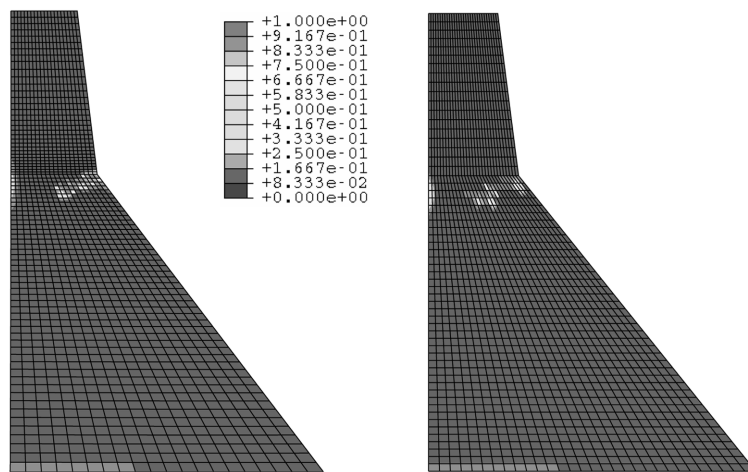


Fig. 8 Effect of meshes size on the distribution of tensile damage in the dam

appears in several elements along the upstream face due to the transverse interaction of dynamic hydropressure. The damage patterns numerically reproduced by the proposed model are consistent with the observed phenomena and those reported by other investigators.

## 6. Conclusions

In this paper, the rate-independent plastic-damage model previously proposed by the authors is first simplified using an empirically-defined evolution law for irreversible strains and then extended into its rate-dependent version to describe the strain rate effect. To characterize the energy dissipation mechanism of structure under dynamic loadings, a new damping model in which a new visco-elastic-damage damping stress due to the vibration is obtained is proposed. It has been illustrated that the proposed damping model reduces to the classical Rayleigh stiffness-proportional damping while the material remains linear-elastic. Also the typical characteristics of the damping in the dynamic nonlinear analysis, e.g., the decreasing damping force resulted from the stiffness degradation of the structure, and the partial restoring of damping due to the unilateral effect upon crack closure, etc., can be well reproduced. Within the framework of continuum damage mechanics, the proposed damping model is incorporated into the rate-dependent plastic-damage model, leading to a unified constitutive model for concrete which is able to directly account for damping on the material scale. Pertinent computational issues concerning the numerical implementation and the algorithmic consistent modulus for the unified model are also discussed in details, through which the dynamic nonlinear analysis of damping structures can be coped with by the same procedures as those without damping.

The proposed unified plastic-damage model is then applied to concrete specimens under different quasi-static and different rate straining loading conditions, and to the Koyna dam under earthquake motions. The predicted results agree fairly well with those from experimental tests and/or other investigators, demonstrating its capability of reproducing most of the typical nonlinear performances of concrete, including the stiffness degradation, the enhancement of strength and ductility under compressive confinement, the strength decay induced by orthogonal tensile cracking, the irreversible deformations upon unloading, the strain rate effect and the damping energy dissipation.

## Acknowledgements

The supports of the Natural Science Foundation for Distinguished Young Scholars of China (Grant No. 59825105) and the Natural Science Foundation for Innovative Researches Groups of China (Grant No.50321803) are gratefully acknowledged.

## References

- Bazant, Z.P. and Oh, B. (1983), "Crack band theory for fracture of concrete", *RILEM Mater. Struct.*, **16**, 155-177.
- Bazant, Z.P. and Pijaudier-Cabot, G. (1988), "Nonlocal continuum damage, localization instability and convergence", *J. Appl. Mech.*, ASME, **55**, 287-293.
- Belytschko, T. *et al.* (1988), "A finite element with embedded localization zones", *Comput. Meth. Appl. Mech. Eng.*, **70**, 59-89.

- Bhattacharjee, S. and Leeger, P. (1993), "Seismic cracking and energy dissipation in concrete gravity dams", *Earthq. Eng. Struct. Dyn.*, **22**, 991-1007.
- Calayir, Y. and Karaton, M. (2005), "A continuum damage concrete model for earthquake analysis of concrete gravity dam-reservoir system", *Soil Dyn. Earthq. Eng.*, **25**, 857-869.
- Cervera, M., Oliver, J. and Manzoli, O. (1996), "A rate-dependent isotropic damage model for the seismic analysis of concrete dams", *Earthq. Eng. Struct. Dyn.*, **25**, 987-1010.
- Comi, C. (1998), "Computational modeling of gradient-enhanced damage in quasi-brittle materials", *Mech. Cohesive-Frictional Mater.*, **4**, 17-36.
- Chopra, A.K. and Chakrabarti, P. (1973), "The Koyna earthquake and the damage to Koyna dam", *Bulletin the Seismological Society America*, **63**(2), 381-397.
- de Borst, R. *et al.* (1995), "On gradient-enhanced damage and plasticity models for failure in quasi-brittle and frictional materials", *Comput. Mech.*, **17**, 130-141.
- El-Aidi, B. and Hall, J. (1989), "Non-linear earthquake response of concrete gravity dams: Part 1: Modeling", *Earthq. Eng. Struct. Dyn.*, **18**, 837-851.
- Faria, R., Oliver, J. and Cervera, M. (1998), "A strain-based plastic viscous-damage model for massive concrete structures", *Int. J. Solids Struct.*, **35**(14), 1533-1558.
- Faria, R., Vila, Pouca, N. and Delgado, R. (2002), "Seismic benchmark of a R/C wall: Numerical simulation and experimental validation", *J. Earthq. Eng.*, **6**(4), 473-498.
- Ghrib, F. and Tinawi, R. (1995), "An application of damage mechanics for seismic analysis of concrete gravity dams", *Earthq. Eng. Struct. Dyn.*, **24**, 157-173.
- Hughes, T.J.R. (1987), *The Finite Element Method*. Prentice-Hall Inc., Englewood Cliffs, New Jersey.
- Jirasek, M. and Zimmermann, T. (2001), "Embedded crack model: I. Basic formulation", *Int. J. Numer. Meth. Eng.*, **50**, 1269-1290.
- Ju, J.W. (1989), "On energy-based coupled elastoplastic damage theories: Constitutive modeling and computational aspects", *Int. J. Solids Struct.*, **25**(7), 803-833.
- Karson, I.D. and Jirsa, J.O. (1969), "Behavior of concrete under compressive loadings", *J. Struct. Div.*, ASCE, **95**(12), 2535-2563.
- Kupfer, H., Hilesdorf, H.K. and Rusch, H. (1969), "Behavior of concrete under biaxial stress", *ACI J.*, **66**, 656-666.
- Lee, J. and Fenves, G.L. (1998), "Plastic-damage model for cyclic loading of concrete structures", *J. Eng. Mech.*, ASCE, **124**, 892-900.
- Li, J. and Wu, J.Y. (2004), "Energy-based CDM model for nonlinear analysis of confined concrete", *ACI SP-238*, In: *Proc. of the Symposium on Confined Concrete*, Changsha, China.
- Lubliner, J., Oliver, S. and Oñate, E. (1989), "A plastic-damage model for concrete", *Int. J. Solids Struct.*, **25**(2), 299-326.
- Mang, H.A. and Hofsetzer, G. (1995), *Computational Mechanics of Reinforced Concrete Structures*. Vieweg Verlag, Braunschweig, Wiesbaden.
- Oliver, J. *et al.* (1990), "Isotropic damage models and smeared crack analysis of concrete", In: *Proc. 2nd Int. Conf. Comp. Aided Analysis Design Conc. Structures*, Zell am See, 945-957.
- Oliver, J. and Simo, J.C. (1994), "Modeling strong discontinuities by means of strain softening constitutive equations", In: *EURO-C 1994 Computer Modeling of Concrete Structures* (Mang, H., Bicanic, N., de Borst, R., editors), Innsbruck, Austria, Pineridge Press: 363-372.
- Oliver, J. (1996), "Modeling strong discontinuities in solids mechanics via strain softening constitutive equation, Part I: Fundamentals; & Part II: Numerical simulation", *Int. J. Numer. Meth. Eng.*, **39**(21), 3575-3623.
- Ortiz, M. (1985), "A constitutive theory for inelastic behavior of concrete", *Mech. Mater.*, **4**, 67-93.
- Ortiz, M., Leroy, Y. and Needleman, A. (1987), "A finite element method for localized failure analysis", *Comput. Meth. Appl. Mech. Eng.*, **61**, 189-214.
- Peerlings, R.H.J. *et al.* (1996), "Gradient-enhanced damage for quasi-brittle materials", *Int. J. Numer. Meth. Eng.*, **39**, 3391-3403.
- Perzyna, P. (1966), "Fundamental problems in viscoplasticity", *Adv. Appl. Mech.* **9**, 244-368.
- Pijaudier-Cabot, G. and Bazant, Z.P. (1987), "Nonlocal damage theory", *J. Eng. Mech.*, **113**, 1512-1533.
- Rots, J.G. (1988), "Computational modeling of concrete fracture", PhD Dissertation, Delft University of

- Technology, Delft.
- Scotta, R. *et al.* (2001), "A scalar damage model with a shear retention factor for the analysis of reinforced concrete structures: Theory and validation", *Comput. Struct.*, **79**, 737-755.
- Simo, J.C. *et al.* (1993), "An analysis of strong discontinuities induced by strain-softening in rate-dependent inelastic solids", *Comput. Mech.*, **12**, 277-296.
- Simo, J.C. and Hughes, T.J.R. (1998), *Computational Inelasticity*, Springer-Verlag, New York.
- Simo, J.C. and Ju, J.W. (1987), "Strain- and Stress-based continuum damage models-I: Formulation", *Int. J. Solids Struct.*, **23**(7), 821-840.
- Suraris, W. and Shah, S.P. (1984), "Rate-sensitive damage theory for brittle solids", *J. Eng. Mech.*, ASCE, **110**, 985-997.
- Vargas-Loli, L. and Fenves, G. (1989), "Effects of concrete cracking on the earthquake response of gravity dams", *Earthq. Eng. Struct. Dyn.*, **18**, 575-592.
- Westergaard, H.M. (1933), "Water pressures on dams during earthquakes", *Transactions the American Society Civil Eng.*, **98**, 418-433.
- Wu, J.Y. and Li, J. (2004), "A new energy-based elastoplastic damage model for concrete", *Proc. of XXI Int. Conf. of Theoretical and Applied Mechanics (ICTAM)*, Warsaw, Poland.
- Wu, J.Y., Li, J. and Faria, R. (2006), "An energy release rate-based plastic damage model for concrete", *Int. J. Solids Struct.*, **43**(3-4), 583-612.
- Yazdani, S. and Schreyer, H.L. (1990), "Combined plasticity and damage mechanics model for plain concrete", *J. Eng. Mech.*, ASCE, **116**(7), 1435-1450.
- Zhang, Q.Y. (2001), "Research on the stochastic damage constitutive of concrete material", Ph.D. Dissertation, Tongji University, Shanghai, China.
- Zienkiewicz, O.C. and Taylor, R. (2000), *The Finite Element Method*. Butterworth-Heinemann, Oxford, 5th edition.

## Appendix: Determination of parameters $A^-$ and $B^-$

Under uniaxial compression, Eq. (36) becomes

$$d^- = 1 - \frac{\varepsilon_0^-}{\varepsilon^{\varepsilon^-}}(1 - A^-) - A^- \exp\left[B^- \left(1 - \frac{\varepsilon^{\varepsilon^-}}{\varepsilon_0^-}\right)\right] \quad (\text{A.1})$$

where  $\varepsilon^{\varepsilon^-}$  denote the elastic strain (positive value) and  $\varepsilon_0^- = f_0^-/E_0$ . Therefore the stress-strain relation under uniaxial compression is expressed as

$$\sigma^- = (1 - d^-)E_0\varepsilon^{\varepsilon^-} = E_0 \left\{ (1 - A^-)\varepsilon_0^- + A^- \varepsilon^{\varepsilon^-} \exp\left[B^- \left(1 - \frac{\varepsilon^{\varepsilon^-}}{\varepsilon_0^-}\right)\right] \right\} \quad (\text{A.2})$$

Therefore introducing the elastic strain  $\varepsilon_p^-$  corresponding to peak strength parameter  $f_c$ ,  $B^-$  is then determined by equating  $d\sigma^-/d\varepsilon^{\varepsilon^-}|_{\varepsilon_p^-} = 0$ , i.e.,

$$\left. \frac{d\sigma^-}{d\varepsilon^{\varepsilon^-}} \right|_{\varepsilon_p^-} = A^- E_0 \exp\left[B^- \left(1 - \frac{\varepsilon_p^-}{\varepsilon_0^-}\right)\right] \left(1 - B^- \frac{\varepsilon_p^-}{\varepsilon_0^-}\right) = 0 \quad (\text{A.3})$$

from which Eq. (38)<sub>2</sub> can be easily obtained.

Substituting Eq. (38)<sub>2</sub> into Eq. (A.2), one obtains the expression for the peak strength  $f_c$

$$f_c = (1 - d_p^-)E_0\varepsilon_p^- = E_0\varepsilon_p^- [(1 - A^-)B^- + A^- \exp(B^- - 1)] \quad (\text{A.4})$$

from which parameter  $A^-$  can be determined as Eq. (38).